



POLİTEKNİK DERGİSİ

*JOURNAL of POLYTECHNIC*

ISSN: 1302-0900 (PRINT), ISSN: 2147-9429 (ONLINE)

URL: <http://dergipark.org.tr/politeknik>



# Physicochemical characterization and filtration performances of waste textile derived carbon -PVDF composite membranes

## *Atık tekstil kaynaklı karbon-PVDF kompozit membranların fizikokimyasal karakterizasyonu ve filtrasyon performansları*

*Author(s): Hüseyin GÜMÜŞ<sup>1</sup>, Bülent BÜYÜKKIDAN<sup>2</sup>,*

*ORCID<sup>1</sup>: 0000-0002-2029-7978*

*ORCID<sup>2</sup>: 0000-0001-9619-3246*

**To cite to this article:** Gümüş H., and Büyükkıdan B., “Physicochemical Characterization and Filtration Performances of Waste Textile Derived Carbon-PVDF Composite Membranes”, *Journal of Polytechnic*, 29(3):290323:1-10 (2026).

**Bu makaleye şu şekilde atıfta bulunabilirsiniz:** Gümüş H., ve Büyükkıdan B., “Physicochemical Characterization and Filtration Performances of Waste Textile Derived Carbon-PVDF Composite Membranes”, *Journal of Polytechnic*, 29(3):290323:1-10 (2026).

**Erişim linki (To link to this article):** <http://dergipark.org.tr/politeknik/archive>

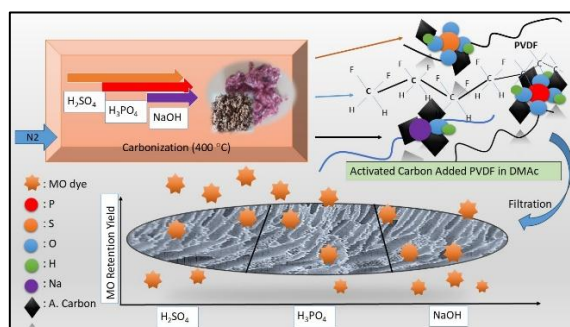
**DOI:** 10.2339/politeknik.1793672

# Physicochemical Characterization And Filtration Performances Of Waste Textile Derived Carbon -PVDF Composite Membranes

## Highlights

- ❖ Non-reusable waste textile consisting of 80% cotton and 20% polyesters was converted into fine chemicals.
- ❖ Functional activated carbons were prepared by pyrolyzing wastes treated with acidic and basic chemicals at 400 °C
- ❖ Dye filtration and fouling resistance of waste textile-based carbon added PVDF composite membranes were investigated.
- ❖ An economical and beneficial alternative solution was presented to burning waste or disposing of it in the environment.

## Graphical Abstract



Şekil. 1 Grafik Özet /Figure. 1 Graphical Abstract

## Aim

This study aims to valorize non-reusable cotton–polyester textile wastes by converting them into chemically modified activated carbons and to evaluate their effectiveness as functional additives in PVDF composite membranes for dye filtration and fouling resistance improvement.

## Design & Methodology

Waste textiles (80% cotton–20% polyester) were chemically impregnated with  $H_2SO_4$ ,  $H_3PO_4$ , and  $NaOH$  and carbonized at 400 °C to obtain functional activated carbons. The prepared carbons were incorporated into PVDF membranes via phase inversion. Structural, chemical, and morphological properties were characterized by XRD, FT-IR, SEM, water uptake, porosity, contact angle, and zeta potential analyses. Filtration performance was evaluated through pure water flux, methyl orange rejection, and multi-cycle fouling resistance tests.

## Originality

This study presents a novel and simple single-step carbonization route for converting waste textile residues into functional activated carbons and demonstrates, for the first time, their direct use as performance-enhancing fillers in PVDF composite membranes for wastewater dye filtration.

## Findings

The incorporation of waste-textile-derived activated carbons significantly altered membrane crystallinity, pore structure, and surface properties. The  $NaOH$ -modified composite exhibited the highest water flux ( $58 L \cdot m^{-2} \cdot h^{-1} \cdot bar^{-1}$ ), while the  $H_3PO_4$ -modified membrane achieved the highest methyl orange rejection (48.2%). All composite membranes showed improved antifouling behavior and higher flux recovery ratios compared to pristine PVDF, with stable performance over repeated filtration cycles.

## Conclusion

Waste textile–derived activated carbon additives effectively enhanced the filtration performance and fouling resistance of PVDF membranes. The proposed approach offers a low-cost, sustainable, and environmentally beneficial alternative to conventional textile waste disposal, highlighting the potential of textile waste valorization for advanced wastewater treatment applications.

## Declaration of Ethical Standards

The authors of this article declare that the materials and methods used in this study do not require ethical committee permission and/or legal-special permission.

# Physicochemical Characterization and Filtration Performances of Waste Textile Derived Carbon-PVDF Composite Membranes

*Araştırma Makalesi / Research Article*

Hüseyin GÜMÜŞ<sup>1\*</sup>, Bülent BÜYÜKKIDAN<sup>2</sup>

<sup>1\*</sup>Osmaneli Vocational School, Bilecik Seyh Edebali University, Turkey

<sup>2</sup>Department of Chemistry, Kutahya Dumlupınar University, Turkey

(Geliş/Received : 30.09.2025 ; Kabul/Accepted : 16.12.2025 ; Erken Görünüm/Early View :03.01.2026 )

## ABSTRACT

In this study, the physicochemical and filtration properties of activated carbon-added polymeric composite membranes were investigated. Additives obtained through the single-step carbonization of waste textile remnants impregnated with H<sub>2</sub>SO<sub>4</sub>, H<sub>3</sub>PO<sub>4</sub>, and NaOH were incorporated into poly(vinylidene fluoride) (PVDF) dissolved in dimethylacetamide (DMAc) by phase inversion. The crystallinity of the prepared composites was analyzed using X-ray diffraction (XRD), while Fourier-transform infrared spectroscopy (FT-IR) was employed to examine molecular interactions. Morphological characterization was performed using scanning electron microscopy (SEM). The water uptake, porosity, and surface hydrophilicity of the membranes were evaluated. Pure water flux and methyl orange (MO) rejection performances were tested using a laboratory-scale filtration system. The NaOH-modified composite (P-KNa) exhibited the highest water flux (58 L·m<sup>-2</sup>·h<sup>-1</sup>·bar<sup>-1</sup>), whereas the H<sub>3</sub>PO<sub>4</sub>-modified composite (P-KH<sub>3</sub>) achieved the highest MO rejection (48.2%). Reversible, irreversible, and total fouling ratios (R<sub>r</sub>, R<sub>i</sub>, and R<sub>t</sub>) were calculated, with the lowest R<sub>t</sub> value (28.5%) observed for P-KNa after three filtration cycles. These findings indicate that the prepared composite membranes possess excellent reusability and are promising candidates for wastewater filtration applications.

**Keywords:** Filtration; Activated carbon; Carbonization; PVDF; Polymeric Composites

## Atık Tekstil Kaynaklı Karbon-PVDF Kompozit Membranların Fizikokimyasal Karakterizasyonu ve Filtrasyon Performansları

### ÖZ

Bu çalışmada, aktif karbon katkılı polimerik kompozit membranların fizikokimyasal ve filtrasyon özellikleri incelenmiştir. H<sub>2</sub>SO<sub>4</sub>, H<sub>3</sub>PO<sub>4</sub> ve NaOH ile emdirilmiş atık tekstil artıklarının tek aşamalı karbonizasyonu ile elde edilen katkı maddeleri, faz inversiyonu yöntemiyle dimetilasetamid (DMAc) içinde çözülmüş poli(viniliden florür) (PVDF) yapısına dahil edilmiştir. Hazırlanan kompozitlerin kristalin yapıları X-ışını kırınımı (XRD) ile analiz edilirken, moleküler etkileşimlerin incelenmesinde Fourier dönüşümlü kızılötesi spektroskopisi (FT-IR) kullanılmıştır. Morfolojik karakterizasyon taramalı elektron mikroskobu (SEM) ile gerçekleştirilmiştir. Membranların su tutma kapasitesi, gözenekliliği ve yüzey hidrofilitliği değerlendirilmiştir. Saf su akışı ve metil oranj (MO) giderim performansları laboratuvar ölçekli bir filtrasyon sistemi kullanılarak test edilmiştir. NaOH ile modifiye edilmiş kompozit (P-KNa) en yüksek su akışını (58 L·m<sup>-2</sup>·h<sup>-1</sup>·bar<sup>-1</sup>) sergilerken, H<sub>3</sub>PO<sub>4</sub> ile modifiye edilmiş kompozit (P-KH<sub>3</sub>) en yüksek MO giderim verimini (%48,2) sağlamıştır. Tersinir, tersinmez ve toplam kirlenme oranları (R<sub>r</sub>, R<sub>i</sub> ve R<sub>t</sub>) hesaplanmış olup, üç filtrasyon çevrimi sonrasında en düşük R<sub>t</sub> değeri (%28,5) P-KNa için gözlemlenmiştir. Bu bulgular, hazırlanan kompozit membranların mükemmel yeniden kullanılabilirliğe sahip olduğunu ve atıksu filtrasyon uygulamaları için umut verici adaylar olduğunu göstermektedir.

**Anahtar Kelimeler:** Filtrasyon; aktif karbon; karbonizasyon; PVDF; polimerik kompozitler

### 1. INTRODUCTION

Membrane-based wastewater treatment enables efficient removal of microbial and chemical contaminants and is commonly enhanced through the incorporation of functional inorganic or polymer-compatible additives. Membranes used in wastewater treatment are generally fabricated from ceramic materials such as Al<sub>2</sub>O<sub>3</sub>, TiO<sub>2</sub>, ZrO<sub>2</sub>, and SiO<sub>2</sub> [1], or from polymeric materials including polysulfone, polyvinylidene fluoride (PVDF), and cellulose acetate [2]. Polymeric composites, which

combine polymers with inorganic or carbon-based fillers, are functional materials possessing large surface areas and tunable acidic-basic active sites. Their optical, electronic, and catalytic properties make them highly useful for water purification, gas separation, and catalysis. Although ceramic membranes exhibit superior thermal and chemical resistance, their high production cost limits their widespread industrial application. Polymeric composites, by contrast, can be manufactured more economically using methods such as phase

\*Sorumlu Yazar (Corresponding Author)  
e-posta: huseyin.gumus@bilecik.edu.tr

inversion, solution casting, solvent evaporation, electrospinning, and melt extrusion [3].

Carbon-enhanced polymeric composites have attracted growing interest as promising filtration materials. Various carbon derivatives, including graphene, graphite, carbon nanotubes (CNTs), and fullerenes—as well as more economical forms such as activated carbon and modified biochar, have been utilized as performance-enhancing fillers [4]. The preparation of these carbon materials typically involves techniques such as pyrolysis, hydrothermal carbonization, gasification, and drying [5]. Activated carbon can be derived from carbon-rich raw materials like agricultural or textile residues under different pyrolysis conditions. For instance, pyrolysis of rice and canola straw at 450 °C produced activated carbon with the highest pore development among temperatures ranging from 250 °C to 650 °C [6]. Similarly, mangrove biomass treated with H<sub>3</sub>PO<sub>4</sub> and carbonized at 300–500 °C achieved optimal adsorption efficiency at an impregnation ratio of 3:1 (H<sub>3</sub>PO<sub>4</sub>: biomass) [7]. Activated carbon prepared at 300 °C with a 4:1 ratio (AC3004) demonstrated a methylene blue adsorption capacity of 72.3 mg/g [8]. Bamboo-derived carbons activated with CO<sub>2</sub> have achieved surface areas up to 1496 m<sup>2</sup>/g [9]. Other biomass sources, such as rice husk, wheat straw, sawdust, sugarcane bagasse, cotton stalks, hemp stalks, coconut leaves, and bamboo have also been explored for activated carbon production under various chemical and thermal conditions [10].

The physicochemical properties of activated carbon can be improved through chemical or physical modification either before (pretreatment) or after carbonization. These modifications enhance adsorption efficiency, energy storage capacity, and other functional properties. For example, selective activated carbon obtained via K<sub>2</sub>CO<sub>3</sub> vapor activation of steam-treated beech coal demonstrated 95% removal efficiency for deoxynivalenol (DON) under optimized conditions [11]. Similarly, palm kernel-based charcoal achieved a xylene adsorption capacity of 23.48 mg/g [12]. The quality of activated carbon depends on precursor composition, heating temperature, reaction duration, and pretreatment procedures. Acid or base washing can remove natural inorganic impurities and improve surface functionality [13]. For instance, phosphate-pretreated wheat straw produced chemically modified activated carbon with superior Pb<sup>2+</sup> adsorption capacity [14].

Biomass-derived activated carbons thus offer an economical and sustainable pathway to produce carbon-rich functional materials. Although powdered activated carbons are effective adsorbents, their recovery and reuse are often limited by separation challenges. Polymeric composites embedding activated carbon particles present a practical alternative and they are easy to handle, mechanically robust, and suitable for repeated use in filtration systems [15]

The textile industry is another major source of carbon-rich waste. Cotton-based textile residues, which contain approximately 40–50% carbon and abundant cellulose,

are ideal precursors for producing value-added carbon materials through carbonization and activation. Transforming such waste into carbon materials contributes simultaneously to waste reduction and environmental remediation. Xu et al. [16] produced magnetic activated carbon from cotton textile waste using FeCl<sub>3</sub> activation optimized through the Box–Behnken design. The optimum conditions (700 °C, 1 h, N<sub>2</sub> atmosphere) yielded 32.7% carbon with a surface area of 837 m<sup>2</sup>/g and a Cr(VI) adsorption capacity of 212.77 mg/g. Similarly, high-surface-area biochar (1167 m<sup>2</sup>/g) prepared from waste cotton woven fabrics using low-dose Fe(NO<sub>3</sub>)<sub>3</sub> activation achieved an adsorption capacity of 456 mg/g for Eriochrome Black T dye [17]. Wannassi et al. [18] converted cotton spinning waste into microporous activated carbon using HNO<sub>3</sub>, H<sub>2</sub>O<sub>2</sub>, and KOH activation at 700 °C. The H<sub>2</sub>O<sub>2</sub>-activated sample (HOAC) exhibited the best performance, with a surface area of 1230 m<sup>2</sup>/g, a total pore volume of 1.20 cm<sup>3</sup>/g, and a sulfur compound adsorption capacity of 168.4 mg/g. These findings confirm that cotton-based textile wastes are excellent feedstocks for synthesizing highly porous activated carbons and biochars. Chemical activation using metal salts (FeCl<sub>3</sub>, Fe(NO<sub>3</sub>)<sub>3</sub>) or oxidizing agents (H<sub>2</sub>O<sub>2</sub>, HNO<sub>3</sub>, KOH) substantially enhances the surface functionality and adsorption capacity of these materials. Consequently, textile waste valorization not only mitigates environmental pollution but also facilitates the development of low-cost, eco-friendly adsorbents for removing heavy metals, organic dyes, and sulfur compounds.

Organic dyes such as methyl orange (MO), methylene blue, Congo red, and malachite green are widely used in various industries and are major contributors to water pollution. Filtration, as an advanced form of adsorption, offers a fast and effective method for removing heavy metals and dyes from aqueous solutions. Methyl orange, an anionic dye at neutral pH, interacts strongly with functional groups on adsorbent and membrane surfaces, making it a suitable model pollutant for evaluating adsorption and antifouling performance [19].

In this study, activated carbon powders were prepared by carbonizing waste textiles composed of 80% cotton and 20% polyester. The waste fabrics were impregnated with H<sub>2</sub>SO<sub>4</sub>, H<sub>3</sub>PO<sub>4</sub>, and NaOH (1:1 mass ratio) and carbonized at 400 °C under optimized conditions. The resulting textile-derived activated carbons were incorporated into PVDF matrices to fabricate composite filtration membranes (designated KH<sub>2</sub>, KH<sub>3</sub>, and KNa-P). The membranes were characterized using XRD, SEM, and FT-IR analyses, and their filtration performance was evaluated through methyl orange removal tests in a custom-designed filtration system. Fouling ratios after three filtration cycles were calculated based on pure water flux measurements. This study, for the first time, explores the feasibility of using carbon-added PVDF composites derived from waste textiles as functional filtration membranes for dye removal and water purification applications.

## 2. MATERIAL and METHOD

H<sub>2</sub>SO<sub>4</sub>, H<sub>3</sub>PO<sub>4</sub> and NaOH modified activated carbons were obtained by carbonization of waste textile remnants in single step carbonization [20]. Analytical grade sodium hydroxide (NaOH, ≥98%), H<sub>2</sub>SO<sub>4</sub> (98%), H<sub>3</sub>PO<sub>4</sub> were obtained and used (from Sigma Aldrich). Methyl orange (MO, or Orange III) was used as a contaminant dye. Polyvinylidene fluoride (PVDF; Solef 6010) membrane material, N,N-Dimethylacetamide (DMAc, 96.18 g.mol<sup>-1</sup>, 0.940 g/mL, ≥99%, Sigma Aldrich) used for solvent. Distilled water was used as phase inversion liquid.

### 2.1. Preparation of Modified Active Carbon Additives

The properties of the activated carbons obtained by carbonization of waste textile are given in Table 1. Modified activated carbon powders using waste textile remnants were prepared as described in our previous study. However, in this study, a new method was developed by differentiating the amount of chemicals and temperature parameters from the previous study [21]. Briefly, textile residues were first removed by washing with ethanol and hot water. 1 mol.L<sup>-1</sup> H<sub>2</sub>SO<sub>4</sub>, H<sub>3</sub>PO<sub>4</sub>, and NaOH solutions were mixed at a 1:1 ratio. Samples transferred to crucibles were heated at 400°C in a nitrogen atmosphere at 5 mL/min for 1 hour to prepare KH2, KH3, and KNa powders. The powders were cooled, washed with distilled water until the pH was neutral, and dried. They were then sieved through a 17-micron sieve to obtain uniform size.

**Table 1.** Properties of activated carbons

Properties	Unit	KH2	KH3	KNa
Iodine Adsorption Number	g/Kg	98.2	113.5	95.9
DBP Adsorption Number	cm <sup>3</sup> /100 g	115.1	154.3	125.2
Pour Density	Kg/m <sup>3</sup>	358	408	265
Heat Loss (moisture)	%	0.42	0.36	0.44
Ash Content	%	1.46	1.64	1.38
pH Value	-	7.1	6.9	7.4
Toluene Discoloration	%	94.2	95.5	91.2
Carbon Content (EDS analysis)	%	81.49	80.86	82.90

### 2.2. Preparation of Modified Active Carbon Added Polymeric Composites

KH2, KH3, KNa anchored PVDF composite membranes were prepared by dissolving of 1.6 g of polymer in 10 mL DMAc. The mixture was stirred at 70 °C for 3 hours. KH2, KH3, KNa powders were added to the polymer solution at the mass ratio of 10% polymer mass. To ensure a homogeneous distribution, the mixtures were kept in an ultrasonic bath for 20 minutes and mixed at 65

°C at 250 rpm for 3 hours to ensure thorough interaction. KH2, KH3, KNa mixed polymer solution was sprouted on glass plate at the thickness of 250 μm (20 cm x 20 cm) and it was immersed in distilled water bath at 25 °C. The polymeric membranes in which phase inversion occurred were kept in water for experimental procedures. Composite membranes with PVDF, 10% KH2, KH3 and KNa additives were named as P, P-KH2, P-KH3 and P-KNa respectively.

### 2.3. Characterization of the Composites

The crystallinity of prepared samples was investigated by XRD; Rigaku 2000, 2°-90° and 5-6°/min scanning speed. Functional groups on the composite membrane were analyzed by automatic 20-scan FT-IR (Perkin Elmer) spectroscopy at 4000-400 cm<sup>-1</sup>. Membrane morphologies were investigated using a scanning electron microscope (SEM, Carl Zeiss ULTRA Plus) at 10 kV. For section images, the composite was first fractured in liquid N<sub>2</sub>. Then, the gold-coated samples were fixed on a carbon holder. In order to interpret the filtration efficiencies of the composites, water uptake capacity (%WU) and porosity (%PO) values were calculated. For this purpose, wet membranes were lightly dried with blotting paper and weighed (W<sub>w</sub>). The membranes were dried in a vacuum oven at 40 °C for two hours and weighed again (W<sub>d</sub>). The tests were carried out 3 times for water uptake and PO% measurements. The WU% values were calculated by equation (1) [22].

$$WU(\%) = \frac{W_w - W_d}{W_w} \times 100 \quad (1)$$

The porosity percentages of the composites (PO%) were calculated by the weight of wet and dry membranes according to equation (2).

$$PO(\%) = \frac{W_w - W_d}{dA\delta} \times 100 \quad (2)$$

Where d is the density of water used at 25 °C, A is the wet membrane area (cm<sup>2</sup>) and δ is the wet membrane thickness by cm unit. The hydrophobicity of composites was explored by the water contact angle (WCA, KSV Attention, Finland) device at 25 °C. After four measurements, WCA was calculated by the in situ drop method and results were calculated by these four measurements. Surface charges of PVDF and composites were measured using zeta potential (Malvern Zetasizer Nano ZS-ZEN 3600 device) in five different pH ranges at 25 °C. The results of automatic measurements made in 3 replicates were recorded in the zeta potential (mV) and total count graph.

### 2.4. Filtration Performances of Composite Membranes

The water flux values (PWF) of P, P-KH2, PKH3 and P-KNa flat sheet composite were determined at ultrafiltration flux system as L.m<sup>-2</sup>.h<sup>-1</sup>.bar<sup>-1</sup>. The filtration pressure (TMP) was set to 0.5, 1.5 and 2 bar. Beforehand, pure water was passed through the membranes for 3

hours to precondition them. PWF was calculated by equation (3):

$$PWF = \frac{V}{At} \quad (3)$$

“V” represents the filtrated volume (L), “A” represents the filtration surface area ( $1.7 \times 10^{-3} \text{ m}^2$ ), and “t” is the time (h). The MO removal efficiencies were determined in the handmade cell. Firstly, the water flux of the membranes was fixed.  $40 \text{ mg.L}^{-1}$  MO was sent into the system. Rejection values were calculated according to equation 3. The flux and rejection experiments were carried out at It was done with new membranes with at least 3 repetitions.

## 2.5. Recycling and Leaching

To test the reusability of the composite membranes, washing was done by  $0.25 \text{ mol.L}^{-1}$  HCl. The presence of metal leaching from the composites to the solution medium was investigated by analyzing the effluent with atomic absorption spectroscopy (AAS, PE, PinAAcle 900 F). The flux recovery ratio (FRR) of the membranes was determined by equation 4.

$$FRR(\%) = \left( \frac{PWF_3}{PWF_1} \right) \times 100 \quad (4)$$

3-run filtration tests using new membranes, the pure water flux values of clean and dirty membranes were measured and the reversible ( $R_r$ ), irreversible ( $R_{ir}$ ) and total fouling ( $R_t$ ) rates were calculated by equations (5-7) [23]:

$$R_r(\%) = \left( 1 - \frac{PWF_2}{PWF_1} \right) \times 100 \quad (5)$$

$$R_{ir}(\%) = \left( 1 - \frac{PWF_3}{PWF_1} \right) \times 100 \quad (6)$$

$$R_t(\%) = \left( 1 - \frac{PWF_2}{PWF_1} \right) \times 100 \quad (7)$$

PWF1 means the pure water flux of the membrane in the first use. PWF<sub>2</sub> and PWF<sub>3</sub> are the water flux values recorded as a result of the second and third use, respectively. Variables such as flux rate, solution concentration, and pH affecting the filtration performance were determined by considering the findings recorded in previous similar studies and used in this study.

## 3.1. Characterization

The  $\alpha$ -phase crystal structure of PVDF was identified from the XRD diffraction pattern, which changed with different additives (Figure 1). The diffraction peaks at  $2\theta = 18.4^\circ$ ,  $20.1^\circ$ , and  $26.6^\circ$ , corresponding to the (020), (110), and (021) crystal planes, respectively, indicate the presence of  $\alpha$ -phase PVDF [24]. These peaks were supported by weaker reflections observed around  $33.2^\circ$ ,  $36.5^\circ$ , and  $41^\circ$ . The intensity of the  $18.4^\circ$  peak in P-KH<sub>2</sub> and P-KNa decreased significantly, indicating an increased formation of amorphous regions. The  $20.6^\circ$  peak, which signifies the presence of the  $\beta$ -phase,

remained relatively strong in P-KNa, while the weak  $36.3^\circ$  peak further supported the existence of the  $\beta$ -phase. The diffraction patterns revealed the coexistence of multiple crystal arrangements whose type and intensity varied depending on the additive used. Another important parameter influencing the crystalline phase is the additive concentration. Furthermore, factors such as polymer solvent, processing temperature, and membrane preparation method also affect phase distribution. It is well established that certain PVDF phases exhibit advantages over others; among them, the  $\beta$ -phase is the most desirable due to its piezoelectric behavior. The formation of this phase can be promoted by appropriate additives [25].

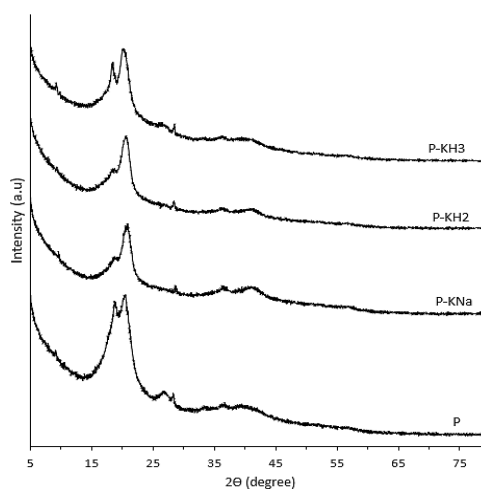


Figure 1. XRD patterns of polymeric composites

The molecular interactions within the composites were analyzed by FT-IR spectroscopy, and the spectra are presented in Figure 2. Characteristic PVDF absorption bands corresponding to C–H, CF<sub>2</sub>, and C–F stretching vibrations were observed at approximately  $875\text{--}1180 \text{ cm}^{-1}$ ,  $1066 \text{ cm}^{-1}$ , and  $1405 \text{ cm}^{-1}$ , respectively [26]. The observed changes in crystal phase distribution with different additives were consistent with the XRD results. The bands at  $976 \text{ cm}^{-1}$  and  $764 \text{ cm}^{-1}$ , associated with the  $\alpha$ -phase chain of PVDF, were clearly visible in the P-KH<sub>2</sub> spectrum but disappeared in the other composites. The bands at  $1275 \text{ cm}^{-1}$  and  $1238 \text{ cm}^{-1}$ , indicative of the  $\beta$ -phase, were evident in P-KH<sub>3</sub> and P-KNa [27].

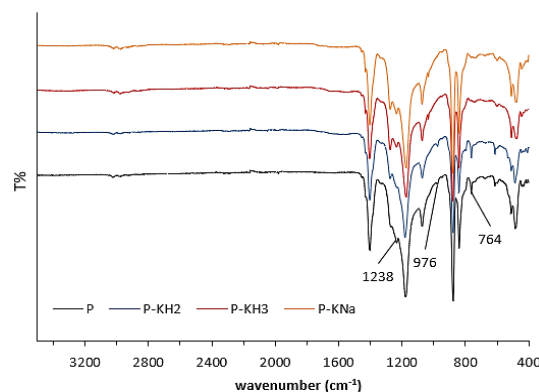


Figure 2. FT-IR spectrums of composites

These findings indicate that the  $\alpha$ -phase structure was transformed into  $\beta$ - and  $\gamma$ -phases, as reflected by the corresponding bands [28]. This transformation demonstrates the significant influence of additive type on the phase arrangement of the polymer chains.

The top-bottom cross-sectional and top-surface SEM images of the modified composites and pristine PVDF are shown in Figure 3. PVDF exhibited a predominantly spongy structure with short finger-like channels on the top surface [29]. In P-KNa, finger-like channels were proportionally formed on both the upper and lower surfaces, displaying symmetrical morphology. In P-KH<sub>2</sub>, finger-like channels extended to approximately half of the membrane thickness (~30  $\mu$ m), whereas in P-KH<sub>3</sub>, compression near the bottom layer hindered the formation of well-defined channels. It is noteworthy that not all additives produce identical effects. For example, LiCl has been reported to exhibit the opposite effect, reducing finger-like macro voids and promoting the development of sponge-like structures [30]. New pore and channel formations associated with additive aggregations were observed in all composites. The differences in additive particle size and non-uniform dispersion resulted in localized defects. Polymer nucleation during phase inversion around these residues affected the shape of the pores and channels. The incorporation of particles into the spongy polymer matrix disrupted the regular pore geometry, leading to narrowing or partial clogging. Factors such as additive-polymer interactions, slurry viscosity, and phase separation rate strongly influence the pore structure of the polymer [31]. As a result, the composites exhibited less permeable yet more selective structures compared to pristine PVDF. Limited imaging was obtained on the dense P-KNa surface due to Na-based agglomerations, whereas P-KH<sub>3</sub> showed a relatively uniform additive distribution and P-KH<sub>2</sub> exhibited larger agglomerates. These results suggest that the modifying chemicals influence the surface functional groups of activated carbon, which in turn affect the crystalline structure and morphology of the polymer through chemical bonding. The proportional additive distribution and internal compression observed in P-KH<sub>3</sub> may be attributed to strong additive-polymer interactions, as supported by the FT-IR spectra.

The surface hydrophilicity, water uptake, and porosity values of pristine PVDF and the composites are presented in Table 2. All membranes exhibited similar hydrophilicity and water uptake properties. This similarity may be attributed to the fact that modification was applied to the activated carbon rather than the polymer itself. Therefore, the effects of sulfate, phosphate, and sodium hydroxide were only partially transferred to the polymer through the activated carbon. However, the highest water uptake capacity was observed in P-KH<sub>2</sub> (65.8  $\pm$  0.8 %), while the highest porosity was obtained for P-KNa (71.2  $\pm$  0.9 %). PVDF is generally preferred for organic matter retention due to

its hydrophobic nature [32]. Numerous factors influence the surface hydrophilicity of PVDF by altering its roughness, including polymer concentration, processing conditions, membrane geometry (fiber, flat sheet, or hollow fiber), and most importantly, the type and ratio of additives [33]. The formation of a dense skin layer reduces surface roughness, thereby increasing hydrophilicity. Nanofillers such as carbon nanotubes, graphene, and other carbon derivatives can effectively fill micro- and nanopores in the polymer, producing a smoother surface and higher hydrophobicity [34, 35].

Because the micro-sized carbon additives filled the voids, all composites exhibited higher surface hydrophobicity than pristine PVDF. The higher hydrophobicity of P-KH<sub>3</sub> compared with PVDF and the other composites was most likely due to the smooth surface formed by active carbon particles filling surface gaps. The flake-like morphology of H<sub>3</sub>PO<sub>4</sub>-modified carbon facilitated the development of a smooth surface in P-KH<sub>3</sub>. Additionally, the upper surfaces of all composites consisted of densely packed and low-permeability pores, a structure particularly advantageous for micro- and sub-micro-filtration applications [36]. The order of smoothness, corresponding to reduced surface roughness, was KH<sub>3</sub> > KNa > KH<sub>2</sub>. Triethyl phosphate has been reported to increase the water contact angle of PVDF membranes prepared via spray-assisted non-solvent-induced phase separation up to 154° [37]. Sulfonated groups have also been used as additives to enhance PVDF hydrophilicity [38]. However, the incorporation and orientation of molecular groups within the polymer during phase inversion depend on multiple factors. The acidic and basic modification agents used in this study generated various functional groups during carbonization of the raw carbon source, some of which are discussed. The KH<sub>3</sub>, KH<sub>2</sub>, and KNa additives interacted molecularly with the polymer and filled interfacial voids during phase inversion, thereby reducing surface roughness.

**Table 2.** WCA, WU% and PO% values of composite membranes

Sample	Water Contact Angle (WCA, °)	WU%	PO%
P	72.3 $\pm$ 3.0	61.7 $\pm$ 1.0	60.9 $\pm$ 0.4
P-KNa	82.7 $\pm$ 3.8	63.6 $\pm$ 0.4	71.2 $\pm$ 0.9
P-KH <sub>3</sub>	86.5 $\pm$ 3.8	60.3 $\pm$ 0.7	68.2 $\pm$ 0.5
P-KH <sub>2</sub>	77.0 $\pm$ 1.0	65.8 $\pm$ 0.8	70.3 $\pm$ 0.8

The recorded changes in the structural properties of the composites emphasize the importance of modified additives. It was demonstrated that the hydrophilicity and pore morphology of membranes two key parameters governing filtration performance can be tuned through additive modification. When the WU % and PO % values of P and P-KH<sub>3</sub> were evaluated together, a noticeable increase in PO % was observed, while WU % changed only slightly. These results suggest the formation of numerous small-sized pores within the composite.

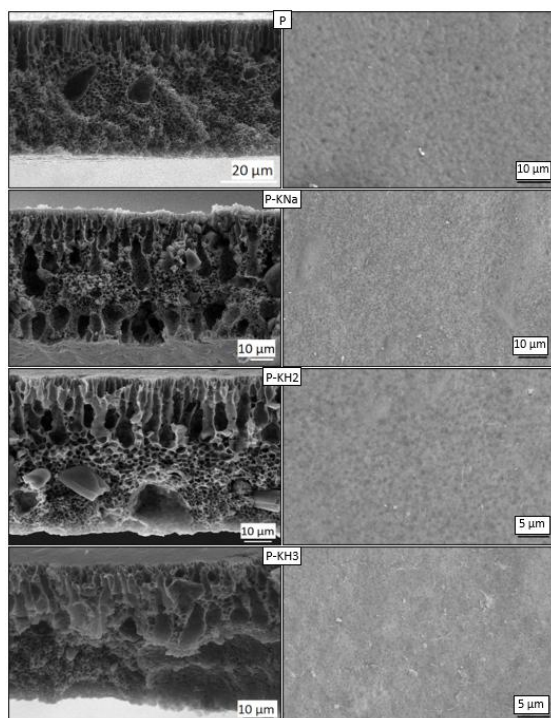


**Figure 3.** Cross-section (left) and surface (right) SEM images of composites

The variations in surface hydrophobicity were consistent with other observed property changes. The increased hydrogen bonding between fluorine atoms in PVDF and oxygen atoms promotes the penetration of water molecules into the pores [39]. However, the presence and distribution of activated carbon within the polymer restricted or altered this interaction, leading to greater water repellency compared to pristine PVDF. While hydrophilicity is advantageous for removing organic contaminants, higher hydrophobicity offers resistance to inorganic fouling. In this study, the modified activated-carbon-based composites displayed beneficially modulated hydrophilic–hydrophobic characteristics [40]. The zeta potentials of P, P-KH<sub>3</sub>, P-KH<sub>2</sub>, and P-KNa were measured to determine their surface charge (Figure 4). The electrical charging behaviors of all samples at different pH levels were similar and consistent with previous studies. Although different chemicals were used for modification, activated carbon remained the dominant component, primarily determining the overall surface charge characteristics. The isoelectric points (IEP) of P, P-KH<sub>2</sub>, and P-KNa were approximately pH 6.5, while P-KH<sub>3</sub> exhibited an IEP above pH 7. The phosphate groups in P-KH<sub>3</sub> showed stronger ion affinity than the other additives, indicating high anion affinity under acidic conditions (pH < 7).

### 3.2. Filtration Efficiencies and Reusing Studies of the Composites

The filtration performance of the flat-sheet composite membranes was evaluated under pressures ranging from 0.5 to 1.5 bar. The pure water flux (PWF) and methyl orange (MO) rejection performances of the membranes

are presented in Figure 5. Among all samples, P-KNa exhibited the highest water flux. The maximum pure water flow rate ( $58 \text{ L} \cdot \text{m}^{-2} \cdot \text{h}^{-1} \cdot \text{bar}^{-1}$ ) was achieved with P-KNa, while the dye rejection efficiency of the composites increased by approximately 73% compared to pristine PVDF (P). The WU % and PO % values provided consistent information regarding the filtration and rejection behavior of the membranes.

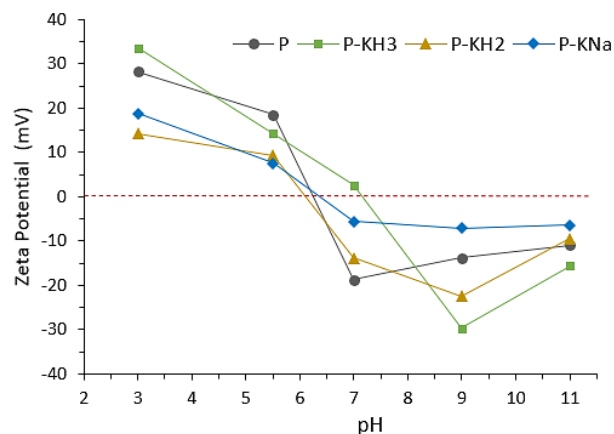


**Figure 4.** Zeta potential curves of composites

It has been demonstrated that a membrane's water-retention capacity largely determines its ion diffusivity (and thus its conductivity) and water uptake. Membranes with higher ion-exchange capacity (IEC) generally exhibit greater water uptake, which enhances ion and water mobility within the membrane matrix. However, excessive water uptake can reduce the influence of fixed charge groups within the membrane (the Donnan effect), thereby decreasing selectivity (e.g., for ion separation) [41]. Overall, the PWF of the composites increased relative to P, except for P-KH<sub>3</sub>. This exception can be explained by the physical structure of P-KH<sub>3</sub>: smaller pores decrease pure water flux, yet the same membrane showed the highest MO rejection (48.2%). A clear correlation was observed between the flux and rejection behavior of P-KNa and P-KH<sub>2</sub>.

Membrane performance is often defined by the trade-off between selectivity and permeability. A more permeable selective layer (thin, swollen, or channeled) generally promotes high water flux but may reduce dye rejection. Therefore, performance cannot be determined solely by pore size, pore geometry, or surface charge. Factors such as concentration polarization (CP), fouling, membrane imperfections, and operating conditions (pressure, flow rate, temperature, pH) also strongly influence the flux–rejection relationship [42]. For instance, thin-film composite (TFC) nanofiltration membranes prepared using a disulfonated diamine co-monomer (S-DADPS) achieved more than 98.5% removal of 100 ppm Cibacron Red and Reactive Orange 16 at all pressures, without significant loss of water flux or salt removal capacity [43].

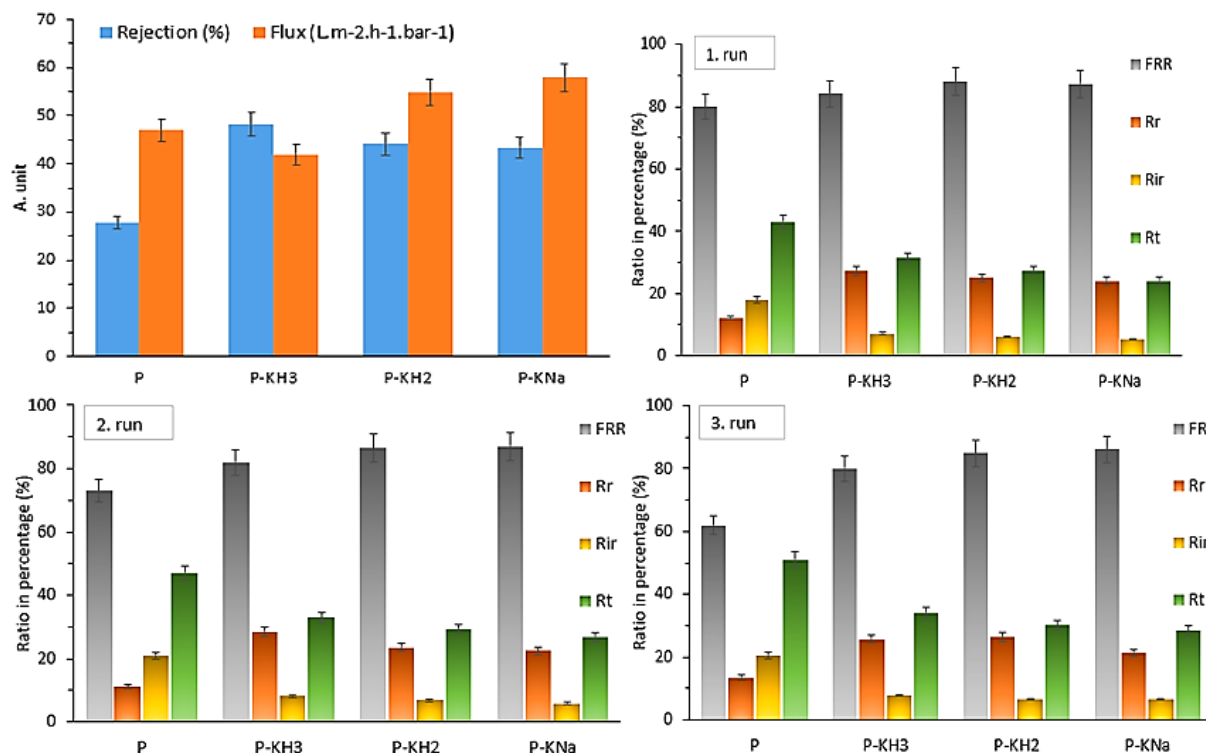


**Figure 5.** Water flux (PWF) and rejection (%) with flux recovery ratio (FRR), reversible (Rr), irreversible (Rir) and total fouling (Rt) of MO filtrated P and composite membranes after 3-run. Filtration parameters= membrane area:  $1.7 \times 10^{-3} \text{ m}^2$ , 1500 mL 40 mg/L MO solution, pressure = 1 bar, MO filtration (1<sup>st</sup> step), filtration after washing (2<sup>nd</sup> and 3<sup>rd</sup> steps).

Smaller pores are generally more susceptible to irreversible (pore-blocking) fouling caused by the entrapment of small particles within the pores, whereas larger pores tend to develop a surface cake layer. The predominant fouling mechanism depends on operating conditions and particle size. Furthermore, factors such as pore-size distribution, hydrodynamic effects, and thermodynamic phenomena (wetting and capillary action) also influence filtration efficiency [44]. Consequently, additives incorporated into the polymer matrix directly affect flux and rejection behavior through their influence on pore formation. Micropores are particularly effective for filtering small molecules, whereas the filtration of large molecules through small pores promotes faster surface accumulation. Therefore, membranes with larger pore structures are more suitable for the removal of large molecules. Filtration efficiency depends not only on pore size but also on the molecular structure of the contaminant and various operational variables. Polymeric materials are particularly valuable because of their tunable chemical and physical properties, and additives serve as functional modifiers that adjust membrane surface characteristics to match the target molecule.

Reusability tests were performed to evaluate the composites' resistance to fouling after multiple filtration cycles. For this purpose, a 1 L solution containing 40 ppm MO was filtered through the membranes. The samples were then washed, and water flux values were re-measured. The flux recovery ratio (FRR) and fouling

behavior were calculated using equations (5–7) based on the water flux values obtained after each cycle. These tests were repeated three times under the same experimental conditions. As shown in Figure 5, the FRR of pristine PVDF decreased significantly after the third use, whereas the FRR of P-KNa and P-KH<sub>2</sub> remained nearly constant. The total fouling rate (R<sub>t</sub>) increased slightly with repeated use but was still lower for all composites than for P.

The additives significantly modified the polymer surface by forming bonds with internal polymer chain sites. In particular, the reduction in surface roughness effectively limited fouling accumulation. The effect of surface roughness varies depending on hydrophobicity or hydrophilicity: increased roughness generally promotes fouling on hydrophobic surfaces but can reduce fouling on hydrophilic ones due to stronger water binding [45]. The model foulant (MO), ionic in nature at neutral pH, possesses charge characteristics similar to the membrane surface, which can influence the extent of fouling. Since pH strongly affects surface charge and electrostatic interactions, filtration under different pH conditions could be investigated in future studies.

Among the composites, P-KH<sub>3</sub> exhibited the highest reversible fouling ratio (R<sub>r</sub>) and an increased total fouling ratio (R<sub>t</sub>). Another key factor contributing to fouling is the nature of the interaction between the membrane surface and the foulant molecules. R<sub>r</sub> represents loosely attached fouling that can be easily removed by rinsing,

while  $R_{ir}$  denotes fouling that adheres to the surface with higher binding energy.

During filtration, accumulations caused by irreversible ( $R_{ir}$ ) and total fouling ( $R_t$ ) block the membrane pores and reduce filtration efficiency. Therefore, the development of materials whose foulants can be easily removed by simple washing has been an important research focus [46]. In the present study, the filtration performance of the composites decreased slightly after multiple filtration cycles, which can be attributed to structural deformation and pore blockage following repeated use. Nevertheless, the prepared composites demonstrated a significantly better antifouling effect compared to the pristine PVDF (P) membrane.

Leaching tests were also conducted to assess potential element release. Calibration solutions in the range of  $1 \times 10^{-3}$ – $1 \times 10^{-5}$  mol·L<sup>-1</sup> were prepared for phosphorus (P), sodium (Na), and sulfur (S) in the filtrate mixture. No metal residues were detected within the mentioned limits, confirming the structural stability and chemical integrity of the composites during operation.

Numerous studies have reported the removal of pesticides, dyes, and pharmaceutical residues using polymeric composites modified with various additives [47]. Parameters such as the functional groups introduced by the additives, the physicochemical properties of the pollutants, and the operational conditions of filtration directly influence removal efficiency. Polymeric composites are often preferred over their pristine forms due to their tunable pore structure and surface characteristics.

Catalyst-modified filtration composites capable of degrading pollutants under light irradiation represent advanced developments in this field. However, even the unmodified filtration efficiencies achieved by the P-KNa, P-KH<sub>3</sub>, and P-KH<sub>2</sub> composites in this study were remarkably high. The modification strategy proposed here offers a simple, low-cost approach that enhances membrane performance by more than 50%, making these materials promising candidates for practical wastewater treatment applications.

PVDF composites modified with H<sub>3</sub>PO<sub>4</sub>, H<sub>2</sub>SO<sub>4</sub>, and NaOH and containing activated carbon were successfully prepared via the phase inversion method. The physicochemical properties of the composites were characterized using XRD, SEM, and FT-IR analyses. Surface hydrophilicity was evaluated through water contact angle, water uptake, and porosity measurements, and surface charge was determined by zeta potential analysis. Activated carbon modified under carbonization conditions played a crucial role in tailoring pore size, hydrophilicity, and surface roughness within the composites.

The filtration performance of the membranes was assessed using a continuous-flux cell by measuring pure water flux and methyl orange (MO) rejection. All composites demonstrated improved performance compared to the pristine PVDF membrane, although the degree of enhancement varied. Among them, P-KH<sub>3</sub>,

which possessed the narrowest pore size distribution, exhibited the highest rejection efficiency (48.2%) but lower pure water flux ( $42 \text{ L} \cdot \text{m}^{-2} \cdot \text{h}^{-1} \cdot \text{bar}^{-1}$ ). The composites also showed enhanced resistance to fouling, one of the major challenges in membrane-based filtration systems. However, the fouling analysis indicated that P-KH<sub>3</sub>, with its smaller pores, experienced the highest degree of surface accumulation among the composites.

The incorporation of chemically modified additives enabled precise control over pore distribution, pore size, and water transport characteristics of the polymer surface. The influence of functional groups introduced by these additives was clearly reflected in the composite performance. Therefore, optimizing processing parameters and additive chemistry is essential for achieving composite membranes with specifically desired structural and functional properties.

#### 4. CONCLUSION

PVDF composites modified with H<sub>3</sub>PO<sub>4</sub>, H<sub>2</sub>SO<sub>4</sub>, and NaOH and containing activated carbon were successfully prepared via the phase inversion method. The physicochemical properties of the composites were characterized using XRD, SEM, and FT-IR analyses. Surface hydrophilicity was evaluated through water contact angle, water uptake, and porosity measurements, and surface charge was determined by zeta potential analysis. Activated carbon modified under carbonization conditions played a crucial role in tailoring pore size, hydrophilicity, and surface roughness within the composites. The filtration performance of the membranes was assessed using a continuous-flux cell by measuring pure water flux and methyl orange (MO) rejection. All composites demonstrated improved performance compared to the pristine PVDF membrane, although the degree of enhancement varied. Among them, P-KH<sub>3</sub>, which possessed the narrowest pore size distribution, exhibited the highest rejection efficiency (48.2%) but lower pure water flux ( $42 \text{ L} \cdot \text{m}^{-2} \cdot \text{h}^{-1} \cdot \text{bar}^{-1}$ ). The composites also showed enhanced resistance to fouling, one of the major challenges in membrane-based filtration systems. However, the fouling analysis indicated that P-KH<sub>3</sub>, with its smaller pores, experienced the highest degree of surface accumulation among the composites. The incorporation of chemically modified additives enabled precise control over pore distribution, pore size, and water transport characteristics of the polymer surface. The influence of functional groups introduced by these additives was clearly reflected in the composite performance. Therefore, optimizing processing parameters and additive chemistry is essential for achieving composite membranes with specifically desired structural and functional properties.

#### DECLARATION OF ETHICAL STANDARDS

The author(s) of this article declare that the materials and methods used in this study do not require ethical committee permission and/or legal-special permission.

## AUTHORS' CONTRIBUTIONS

**Huseyin Gumus:** Conceptualization, Supervision, Writing-Original draft preparation.

**Bulent Buyukkidan:** Investigation, Resources, Visualization, Data curation, Validation

## CONFLICT OF INTEREST

There is no conflict of interest in this study.

## REFERENCES

- [1] Asif, M. B., Zhang, Z. "Ceramic membrane technology for water and wastewater treatment: A critical review of performance, full-scale applications, membrane fouling and prospects". *Chem. Eng. J.* 418:129481 (2021).
- [2] Iqbal, A., Cevik, E., Mustafa, A., Qahtan, T. F., Zeeshan, M., Bozkurt, A. "Emerging developments in polymeric nanocomposite membrane-based filtration for water purification: A concise overview of toxic metal removal". *Chem. Eng. J.* 481:148760 (2024).
- [3] Yılmaz, M., Öztürk, E. "İnorganik katkı içeren polimer kompozit membranların üretimi ve performans analizi". *Politeknik Dergisi.* 24:1293–1302 (2021).
- [4] Petukhov, D. I., Johnson, D. J. "Membrane modification with carbon nanomaterials for fouling mitigation: A review". *Adv. Colloid Interface Sci.* 327:103140 (2024).
- [5] Cuong, D. V., Matsagar, B. M., Lee, M., Hossain, Md. S. A., Yamauchi, Y., Vithanage, M., Sarkar, B., Ok, Y. S., Wu, K. C.-W., Hou, C.-H. "A critical review on biochar-based engineered hierarchical porous carbon for capacitive charge storage". *Renew. Sustain. Energy Rev.* 145:111029 (2021).
- [6] Yaashikaa, P. R., Kumar, P. S., Varjani, S., Saravanan, A. "A critical review on the biochar production techniques, characterization, stability and applications for circular bioeconomy". *Biotechnol. Rep.* 28:e00570 (2020).
- [7] Zakaria, R., Jamalluddin, N. A., Abu Bakar, M. Z. "Effect of impregnation ratio and activation temperature on the yield and adsorption performance of mangrove based activated carbon for methylene blue removal". *Results Mater.* 10:100183 (2021).
- [8] Yang, C., Liu, J., Lu, S. "Pyrolysis temperature affects pore characteristics of rice straw and canola stalk biochars and biochar-amended soils". *Geoderma.* 397:115097 (2021).
- [9] Khuong, D. A., Nguyen, H. N., Tsubota, T. "Activated carbon produced from bamboo and solid residue by CO<sub>2</sub> activation utilized as CO<sub>2</sub> adsorbents". *Biomass Bioenergy.* 148:106039 (2021).
- [10] Haider, R., Sagadevan, S., Cameron, N. R., Johan, M. R. "Biomass-derived activated carbon for high-performance energy storage devices". *J. Power Sources.* 633:236404 (2025).
- [11] Müller, B. "Preparation and characterization of K<sub>2</sub>CO<sub>3</sub>-doped powdered activated carbon for effective in-vitro adsorption of deoxynivalenol". *Bioresour. Technol. Rep.* 15:100703 (2021).
- [12] Pazira, R., Lashanizadegan, A., Sharififard, H., Darvishi, P. "Xylene removal from dilute solution by palm kernel activated charcoal: *Kinetics and equilibrium analysis.* 2:107-117 (2018).
- [13] Yuan, Z., Xu, Z., Zhang, D., Chen, W., Huang, Y., Zhang, T., Tian, D., Deng, H., Zhou, Y., Sun, Z. "Mesoporous activated carbons synthesized by pyrolysis of waste polyester textiles mixed with Mg-containing compounds and their Cr(VI) adsorption". *Colloids Surf. Physicochem. Eng. Asp.* 549:86-93 (2018).
- [14] Miao, X., Lin, J., Bian, F. "Utilization of discarded crop straw to produce cellulose nanofibrils and their assemblies". *J. Bioresour. Bioprod.* 5:26-36 (2020).
- [15] Duman, A., Yıldırım, S. "Biyokütle kaynaklı aktif karbon katkılı polimer kompozit membranların hazırlanması ve adsorpsiyon performanslarının incelenmesi," *Politeknik Dergisi,* 26: 1421–1430 (2023).
- [16] Xu, Z., Wang, Y., Wu, M., Chen, W. "Preparation of biochar derived from waste cotton woven by low-dosage Fe(NO<sub>3</sub>)<sub>3</sub> activation: characterization, pore development, and adsorption". *Environ. Sci. Pollut. Res.* 30:49523-49535 (2023).
- [17] Xu, Z., Zhang, T., Yuan, Z., Zhang, D., Sun, Z., Huang, Y., Chen, W., Tian, D., Deng, H., Zhou, Y. "Fabrication of cotton textile waste-based magnetic activated carbon using FeCl<sub>3</sub> activation by the Box–Behnken design: optimization and characteristics". *RSC Adv.* 8:38081-38090 (2018).
- [18] Wannassi, B., Kanan, M., Hariz, I. B., Assaf, R., Abusaq, Z., Ben Hassen, M., Aljazzar, S., Zahran, S., Khouj, M. T., Barham, A. S. "Cotton Spinning Waste as a Microporous Activated Carbon: Application to Remove Sulfur Compounds in a Tunisian Refinery Company". *Sustainability.* 15 (2023).
- [19] Güneş, A., Koyuncu, M. "Sulu çözümlerden metil oranj ve metilen mavisinin adsorpsiyon yoluyla giderimi: kinetik ve izoterm incelemesi," *Politeknik Dergisi,* 25:839-848 (2022).
- [20] Gumus, H., Buyukkidan, B. "A Simple and Green Preparation Route of Waste Textile Based Photocatalytic Biochars for Pollution Removal". *Chem. Afr.* 6:629–642 (2023).
- [21] Gumus, H., Buyukkidan, B. "Karbonize Edilmiş Tekstil Atığı Katkılı Poli(Vinil Florür) Kompozitlerin Üretimi ve Karakterizasyonu. In *Matematik ve Fen Alanında Uluslararası Araştırmalar VI. Eğitim Yayın Evi.* 119-130 (2022).
- [22] Isloor, A., Pereira, V., Bhat, B., Al-Obaid, A., Fun, H., Ismail, A. "Preparation and performance studies of Polysulfone-Sulfated nano-Titania (S-TiO<sub>2</sub>) nanofiltration membranes for dye removal". *RSC Adv.* 5 (2015).
- [23] Chen, Z., Chen, G.-E., Xie, H.-Y., Xu, Z.-L., Li, Y.-J., Wan, J.-J., Liu, L.-J., Mao, H.-F. "Photocatalytic antifouling properties of novel PVDF membranes improved by incorporation of SnO<sub>2</sub>-GO nanocomposite for water treatment". *Sep. Purif. Technol.* 259:118184 (2021).
- [24] Cai, X., Lei, T., Sun, D., Lin, L. "A critical analysis of the  $\alpha$ ,  $\beta$  and  $\gamma$  phases in poly(vinylidene fluoride) using FTIR". *RSC Adv.* 7:15382-15389 (2017).
- [25] Brunengo, E., Luciano, G., Canu, G., Canetti, M., Conzatti, L., Castellano, M., Stagnaro, P. "Double-step moulding: An effective method to induce the formation of  $\beta$ -phase in PVDF". *Polymer.* 193:122345 (2020).
- [26] Uličná, S., Owen-Bellini, M., Moffitt, S. L., Sinha, A., Tracy, J., Roy-Choudhury, K., Miller, D. C., Hacke, P., Schelhas, L. T. "A study of degradation mechanisms in PVDF-based photovoltaic backsheets". *Sci. Rep.* 12:14399 (2022).
- [27] Mireja, S., Khakhar, D. V. "High  $\beta$  phase PVDF films formed by uniaxial compression". *Polymer.* 293:126665 (2024).

- [28] María, N., Maiz, J., Rodionov, V., Hadjichristidis, N., Müller, A. J. "4-Miktoarm star architecture induces PVDF  $\beta$ -phase formation in (PVDF)<sub>2</sub>-b-(PEO)<sub>2</sub> miktoarm star copolymers". *J Mater Chem C*. 8:13786-13797 (2020).
- [29] Wang, Z., Ma, J., Liu, Q. "Pure sponge-like membranes bearing both high water permeability and high retention capacity". *Desalination*. 278:141-149 (2011).
- [30] Kim, C.-H., Yoo, Y., Ayode Otitoju, T., Kim, I.-C., Nam, S.-E., Park, Y.-I., Cho, Y. H. "Controlling the polymorphs of PVDF membranes: Effects of a salt additive on PVDF polarization during phase separation processes". *Sep. Purif. Technol.* 351:128120 (2024).
- [31] Su, J. F., Beltsios, K. G., Li, P.-H., Cheng, L.-P. "Facile formation of symmetric microporous PVDF membranes via vapor-induced phase separation of metastable dopes". *Colloids Surf. Physicochem. Eng. Asp.* 634:128012 (2022).
- [32] M.Hamad, E., Al-Gharabli, S., Kujawa, J. "Tunable hydrophobicity and roughness on PVDF surface by grafting to mode – Approach to enhance membrane performance in membrane distillation process". *Sep. Purif. Technol.* 291:120935 (2022).
- [33] Atakul, T., Güneş, E. ve Karataş, S., "Production of PVDF-based filters for dye removal from water and determining its effectiveness through experimental optimization for the adsorption," *Politeknik Dergisi*, 27:1249–1258, (2024).
- [34] Zakaria, N. A., Zaliman, S. Q., Leo, C. P., Ahmad, A. L., Ooi, B. S., Poh, P. E. "Electrochemical cleaning of superhydrophobic polyvinylidene fluoride/polymethyl methacrylate/carbon black membrane after membrane distillation". *J. Taiwan Inst. Chem. Eng.* 138:104448 (2022).
- [35] Özden Yenigün, E. "Karbon Nanotüp-Polimer Nanokompozitlerde Çok Boyutlu Modelleme ile Arayüz Özelliklerinin İncelenmesi". *Politek. Derg.* 20:503-511 (2017).
- [36] Akduman, Ç. "PVDF Electrospun Nanofiber Membranes for Microfiltration: The Effect of Pore Size and Thickness on Membrane Performance". *Avrupa Bilim Ve Teknol. Derg.* 247-255 (2019). doi:10.31590/ejosat.556748.
- [37] Yang, H.-R., Huang, Y.-H., Wang, C.-F., Chung, T.-S. "Green fabrication of PVDF superhydrophobic membranes using a green solvent triethyl phosphate (TEP) for membrane distillation". *Desalination*. 566:116934 (2023).
- [38] Kumar, V., Rudra, R., Hait, S. "Sulfonated polyvinylidene fluoride-crosslinked-aniline-2-sulfonic acid as ion exchange membrane in single-chambered microbial fuel cell". *J. Environ. Chem. Eng.* 9:106467 (2021).
- [39] Chen, S., Yao, K., Tay, F., Liow, C. "Ferroelectric Poly(Vinylidene Fluoride) Thin Films on Si Substrate with the Beta Phase Promoted by Hydrated Magnesium Nitrate". *J. Appl. Phys.* 102:104108-104108 (2007).
- [40] Shah, L. A., Malik, T., Siddiq, M., Haleem, A., Sayed, M., Naeem, A. "TiO<sub>2</sub> nanotubes doped poly(vinylidene fluoride) polymer membranes (PVDF/TNT) for efficient photocatalytic degradation of brilliant green dye". *J. Environ. Chem. Eng.* 7:103291 (2019).
- [41] Sireci, E., Luca, G. D., Salvo, J. L. D., Cipollina, A., Micale, G. "Prediction of equilibrium water uptake and ions diffusivities in ion-exchange membranes combining molecular dynamics and analytical models". *J. Membr. Sci.* 668:121283 (2023).
- [42] D'Haese, A., Yaroshchuk, A. "Interplay between membrane imperfections and external concentration polarization". *J. Membr. Sci.* 676:121579 (2023).
- [43] Ormanci-Acar, T., Tas, C. E., Keskin, B., Ozbulut, E. B. S., Turken, T., Imer, D., Tufekci, N., Menciloglu, Y. Z., Unal, S., Koyuncu, I. "Thin-film composite nanofiltration membranes with high flux and dye rejection fabricated from disulfonated diamine monomer". *J. Membr. Sci.* 608:118172 (2020).
- [44] Zhao, F., Han, X., Shao, Z., Li, Z., Li, Z., Chen, D. "Effects of different pore sizes on membrane fouling and their performance in algae harvesting". *J. Membr. Sci.* 641:119916 (2022).
- [45] Zhao, D., Chen, L., Peng, M., Xue, B., Yao, Z., Huang, W., Wang, Z., Liu, J. "The complex influence of membrane roughness on colloidal fouling: A dialectical perspective". *J. Membr. Sci.* 725:124014 (2025).
- [46] Ounifi, I., Guesmi, Y., Ursino, C., Santoro, S., Mahfoudhi, S., Figoli, A., Ferjanie, E., Hafiane, A. "Antifouling Membranes Based on Cellulose Acetate (CA) Blended with Poly(acrylic acid) for Heavy Metal Remediation". *Appl. Sci.* 11:4354 (2021).
- [47] Hani, U. "Comprehensive review of polymeric nanocomposite membranes application for water treatment". *Alex. Eng. J.* 72:307-321 (2023).